

# Novel Multilevel Inverter Carrier-Based PWM Methods

Leon M. Tolbert  
 Oak Ridge National Laboratory  
 P.O. Box 2009, Bldg. 9102-1  
 Oak Ridge, TN 37831-8038  
 Tel: (423) 576-6206  
 E-mail: tolbertlm@ornl.gov

Thomas G. Habetler  
 Georgia Institute of Technology  
 School of Electrical and Computer Engineering  
 Atlanta, GA 30332-0250  
 Tel: (404) 894-9829  
 E-mail: tom.habetler@ece.gatech.edu

**Abstract** The advent of the transformerless multilevel inverter topology has brought forth various pulse width modulation (PWM) schemes as a means to control the switching of the active devices in each of the multiple voltage levels in the inverter. An analysis of how existing multilevel carrier-based PWM affect switch utilization for the different levels of a diode-clamped inverter is conducted. Two novel carrier-based multilevel PWM schemes are presented which help to optimize or balance the switch utilization in multilevel inverters. A 10 kW prototype six-level diode-clamped inverter has been built and controlled with the novel PWM strategies proposed in this paper to act as a voltage source inverter.

## I. INTRODUCTION

Multilevel pulse width modulation (PWM) inverters have been developed to overcome shortcomings in solid state switching device ratings so that large motors can be controlled by high-power adjustable frequency drives. The most popular structure proposed as a transformerless voltage source inverter is the diode clamped converter based on the neutral point converter proposed by Nabae [1]. A three-phase 6-level diode-clamped inverter is shown in Fig. 1.

The two multilevel PWM methods most discussed in the literature are multilevel carrier based PWM and multilevel space vector PWM; both are extensions of traditional two-level PWM strategies to several levels. Investigators have proposed carrier-based multilevel sine-triangle PWM schemes for control of a multilevel diode clamped inverter used as a motor drive or static var compensator [2-9]. Others have generalized space vector PWM theory for use with multilevel inverters [10-12]. A third PWM method used to control a multilevel diode clamped converter is with selective harmonic elimination [13-14].

While the multilevel PWM techniques developed thus far have been extensions of two-level PWM methods, the multiple levels in a diode-clamped inverter offer extra degrees of freedom and greater possibilities in terms of device

Prepared by the Oak Ridge National Laboratory, Oak Ridge, Tennessee 37831-8038, managed by Lockheed Martin Energy Research, Corp. for the U.S. Department of Energy under contract DE-AC05-96OR22464. A contractor of the U.S. Government has authored the submitted manuscript. Accordingly, the U.S. Government retains a nonexclusive, royalty-free license to publish or reproduce the published form of this contribution, or allow others to do so, for U.S. Government purposes.

utilization, state redundancies, and effective switching frequency. In this paper, novel carrier-based multilevel PWM schemes are presented which take advantage of the special properties available in multilevel inverters to minimize switch utilization and/or balance the switching duty among its various levels.

## II. EXISTING MULTILEVEL CARRIER-BASED METHODS

### A. Subharmonic PWM Method

Other authors have extended two-level carrier based PWM techniques to multilevel inverters by making the use of several triangular carrier signals and one reference signal per phase. Carrara [3] developed multilevel subharmonic PWM (SH-PWM) as follows. For an  $m$ -level inverter,  $m-1$  carriers with the same frequency  $f_c$  and same peak-to-peak amplitude  $A_c$  are disposed such that the bands they occupy are contiguous. The reference, or modulation, waveform has peak-to-peak amplitude  $A_m$  and frequency  $f_m$ , and it is centered in the middle of the carrier set. The reference is continuously compared with each of the carrier signals. If the reference is greater than a carrier signal, then the active

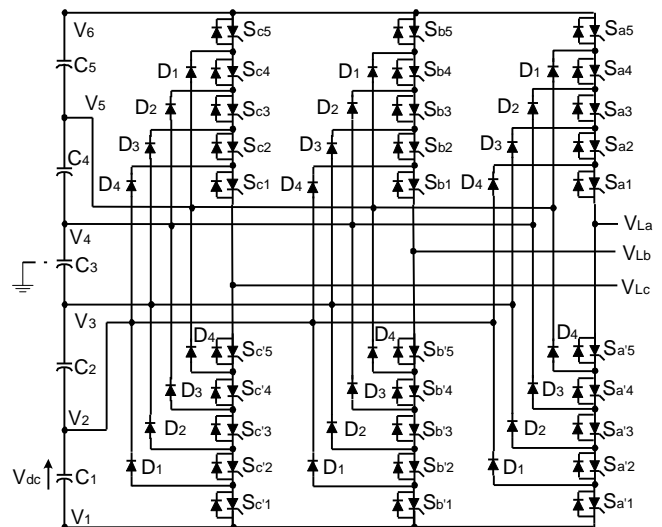


Fig. 1. Circuit diagram of a three-phase 6-level diode clamped inverter.

device corresponding to that carrier is switched on; and if the reference is less than a carrier signal, then the active device corresponding to that carrier is switched off. In multilevel inverters, the amplitude modulation index,  $m_a$ , and the frequency ratio,  $m_f$ , are defined as

$$m_a = \frac{A_m}{(m-1) \cdot A_c}, \quad (1)$$

$$m_f = \frac{f_c}{f_m}. \quad (2)$$

Carrara also considered different methods of disposing the many carrier bands required in multilevel PWM. The three cases he considered for an inverter with an odd number of levels were as follows:

1. Alternative phase opposition disposition where each carrier band is shifted by 180 degrees from the adjacent bands.
  2. Phase opposition disposition where the carriers above the zero reference are in phase but shifted by 180 degrees from those carriers below the zero reference.
  3. In phase disposition where all the carriers are in phase.
- Further examination of in phase disposition is given in this paper.

Fig. 2 shows a set of carriers ( $m_f = 21$ ) with all of the carriers in phase for a 6-level diode-clamped inverter and a sinusoidal reference voltage with a modulation index of 0.8. The resulting output voltage of the inverter is also shown in Fig. 2.

### B. Switching Frequency Optimal PWM Method

Steinke [2] proposed a carrier-based method termed switching frequency optimal PWM (SFO-PWM) which was similar to Carrara's except that a zero sequence (triplen harmonic) voltage is added to each of the carrier waveforms. This method takes the instantaneous average of the maximum and minimum of the three reference voltages ( $V_a^*, V_b^*, V_c^*$ )

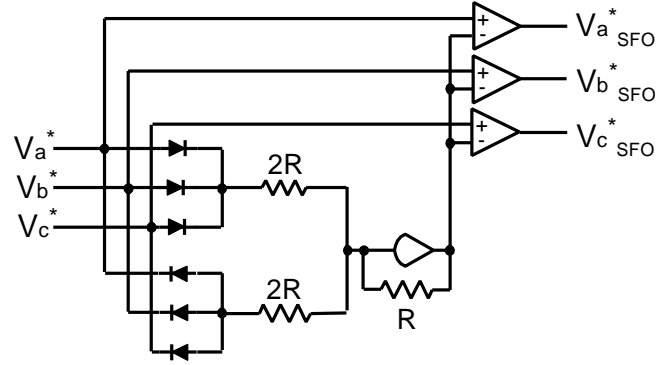


Fig. 3. Analog equivalent circuit for SFO-PWM zero sequence addition.

and subtracts this value from each of the individual reference voltages to obtain the modulation waveforms, i.e.,

$$V_{offset} = \frac{\max(V_a^*, V_b^*, V_c^*) + \min(V_a^*, V_b^*, V_c^*)}{2}, \quad (3)$$

$$\begin{aligned} V_{a\ SFO}^* &= V_a^* - V_{offset}, \\ V_{b\ SFO}^* &= V_b^* - V_{offset}, \\ V_{c\ SFO}^* &= V_c^* - V_{offset}. \end{aligned} \quad (4)$$

The addition of this triplen-offset voltage continuously centers all of the three reference waveforms in the carrier band, which Holmes [15] showed for carrier-based two-level PWM is similar to using space vector PWM with the zero voltage state divided evenly at the beginning and end of each half carrier interval. The analog equivalent of (3) and (4) is shown in Fig. 3.

SFO-PWM is illustrated in Fig. 4 for the same reference voltage waveform that was used in Fig. 2. The resulting output voltage of the inverter is also shown in Fig. 4. The SFO-PWM technique can only be used for three-phase three-wire systems, and it enables the modulation index to be increased by 15% before overmodulation occurs.

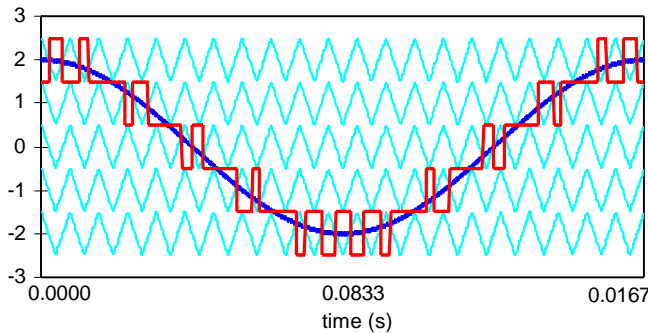


Fig. 2. Multilevel carrier-based SH-PWM showing carrier bands, modulation waveform, and inverter output waveform ( $m = 6$ ,  $m_f = 21$ ,  $m_a = 0.8$ ).

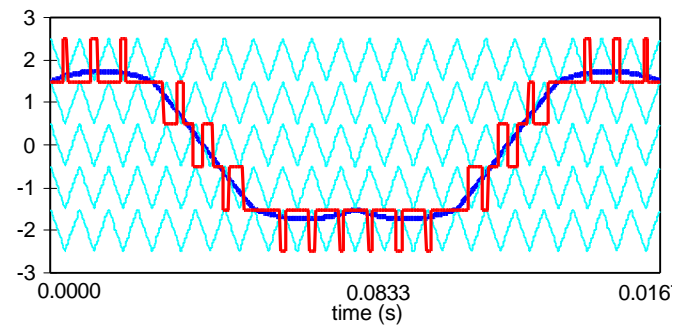


Fig. 4. Multilevel carrier-based SFO-PWM showing carrier bands, modulation waveform, and inverter output waveform ( $m = 6$ ,  $m_f = 21$ ,  $m_a = 0.8$ ).

### III. CARRIER PHASE ANGLE EFFECT ON SWITCHING

Previously, Menzies [5] considered two simple cases of what effect the displacement phase angle,  $\mathbf{f}$ , between the modulation waveform (sinusoidal reference) and the carrier waveforms, has on the switching of the active devices and the unfiltered inverter output waveform distortion where

$$V_a^* = |V| \cdot \cos(\mathbf{q} - \mathbf{f}). \quad (5)$$

The two cases considered were 1) the carrier is a maximum when the reference is a maximum ( $\mathbf{f} = 0$ ), referred to as a W-type carrier set, and 2) the case where the carrier is a minimum when the reference is a maximum, referred to as a M-type carrier set.

In this paper, all displacement phase angles were considered. The displacement phase angle between the reference and carrier set was varied incrementally by 0.01 radians from 0 to  $\pi/3$  radians (120 degrees) to see what effect this would have on the total switchings of the active devices and the output waveform distortion.

In Fig. 5, an example of controlling a 6-level inverter with the SH-PWM method, with  $m_a = 0.8$  and  $m_f = 21$ , shows that the total number of switchings (active device transition from on-to-off or off-to-on),  $N_{sw}$ , during a modulation cycle,  $1/f_m$ , can vary between 34 and 50 depending on the phase angle of the reference. Although the waveforms are not quarter-wave symmetric for some values of  $\mathbf{f}$ , the waveforms are always half-wave symmetric regardless of the displacement angle. Note that in a traditional two-level inverter with a single carrier wave,  $N_{sw} = 42$  for  $m_f = 21$  regardless of the displacement phase angle and for all values of  $m_a < 1$ .

Table I shows the number of switchings at each level of the diode-clamped inverter for the examples shown in Fig. 5. The upper and lower main device pairs ( $S_{a1} - S_{a'1}$ ,  $S_{a5} - S_{a'5}$ , in a 6-level inverter), in general, are switched more often than the intermediate switches for carrier-based control where each level has the same carrier frequency.

In Fig. 6, an example with a 6-level inverter with the SFO-PWM method and the same parameters as Fig. 5 shows that the total number of switchings can vary between 30 and 46. Table II shows the number of switchings at each level of the inverter for the examples represented in Fig. 6. Again, and

even more dramatically, the upper and lower main device pairs are switched more often than the intermediate switches.

Fig. 7 shows the frequency spectrum for the unfiltered output phase voltage shown in Fig. 5(a) ( $\mathbf{f}=0.00$  rad,  $N_{sw} = 34$ ) and Fig. 5(e) ( $\mathbf{f}=0.15$  rad,  $N_{sw} = 50$ ). From these frequency spectrums, one can see that the dominant harmonic in the phase voltage ( $21^{st}$ ) is the carrier ratio  $m_f$ . This illustrates the importance of choosing the carrier ratio to be a triplen such that this harmonic does not show up in the line-line voltage because it cancels out [3, 4].

One can also see that the only difference in the frequency spectrum for the two different displacement angles is in the magnitude of the harmonics whose order is above the carrier ratio ( $m_f = 21$ ). The magnitude of the harmonics whose order is below the carrier ratio is nearly identical for the two cases.

An algorithm was written to count the total number of switchings during a modulation cycle with varying values of  $\mathbf{f}$  for  $m_f$  from 9 to 39 for the SH-PWM and SFO-PWM cases where  $m_a = 0.8$  and  $m = 6$ . Some interesting observations have been gleaned from these simulations:

1. If the carrier ratio  $m_f$  is a multiple of 16, the phase angle between the carrier and reference has no effect on the total number of switchings, i.e.,  $N_{sw}$  does not vary with  $\mathbf{f}$ .
2. If the carrier ratio  $m_f$  is even (multiple of 2), then the maximum number of switchings for a modulation cycle is  $2m_f$  and  $N_{sw} = 2m_f - 2j$  where  $j = 0, 1, 2, 3$  (exact values for  $j$  depend on the ratio  $m_f$ ).
3. If the carrier ratio  $m_f$  is odd, then the maximum number of switchings for a modulation cycle is *greater* than  $2m_f$  and  $N_{sw} = 2m_f + 4j$  where  $j = -2, -1, 0, 1, 2$  (exact values for  $j$  depend on the ratio  $m_f$ ).

These points show a major difference between two-level PWM and multilevel PWM. In *two-level PWM*, the switching frequency is *always equal* to the carrier frequency for modulation indices less than unity. In *multilevel PWM*, the switching frequency can be *less than or greater than* the carrier frequency and *is a function of the displacement angle between the carrier set and the modulation waveform*. By choosing a phase displacement angle that minimizes the number of active device switchings for a particular  $m_a$  and  $m_f$ , switching losses can be reduced by as much as 35%, which increases the efficiency of the inverter considerably.

TABLE I

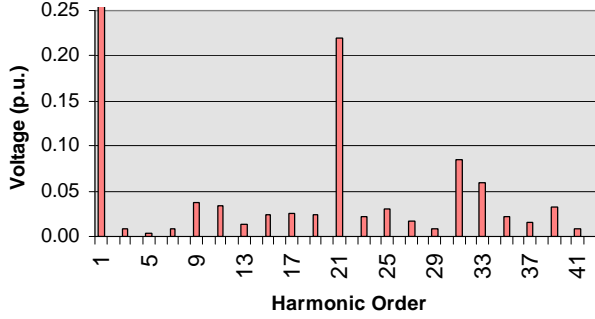
NUMBER OF MAIN DEVICE SWITCHINGS IN EACH LEVEL FOR FIG. 5

Carrier Phase Angle, $\mathbf{f}$	Switches per Cycle (SH-PWM, $m = 6$ , $m_f = 21$ , $m_a = 0.8$ )					
	$S_{a1}, S_{a'1}$	$S_{a2}, S_{a'2}$	$S_{a3}, S_{a'3}$	$S_{a4}, S_{a'4}$	$S_{a5}, S_{a'5}$	$N_{sw}$
0.00 rad	8	6	6	6	8	34
0.03 rad	10	6	6	6	10	38
0.08 rad	10	8	6	8	10	42
0.13 rad	10	8	10	8	10	46
0.15 rad	10	10	10	10	10	50

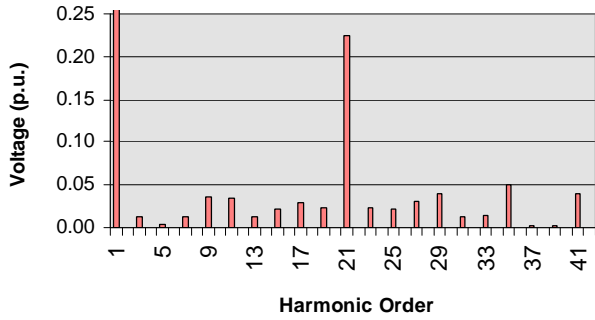
TABLE II

NUMBER OF MAIN DEVICE SWITCHINGS IN EACH LEVEL FOR FIG. 6

Carrier Phase Angle, $\mathbf{f}$	Switches per Cycle (SFO-PWM, $m = 6$ , $m_f = 21$ , $m_a = 0.8$ )					
	$S_{a1}, S_{a'1}$	$S_{a2}, S_{a'2}$	$S_{a3}, S_{a'3}$	$S_{a4}, S_{a'4}$	$S_{a5}, S_{a'5}$	$N_{sw}$
0.03 rad	14	6	6	6	14	46
0.08 rad	14	4	6	4	14	42
0.11 rad	14	4	2	4	14	38
0.13 rad	12	4	2	4	12	34
0.15 rad	12	2	2	2	12	30



(a) SH-PWM,  $m_f = 21$ ,  $m_a = 0.8$ ,  $f = 0.00$  rad,  $N_{sw} = 34$



(b) SH-PWM,  $m_f = 21$ ,  $m_a = 0.8$ ,  $f = 0.15$  rad,  $N_{sw} = 40$

Fig. 7. Frequency spectrum of unfiltered output phase voltage waveform. (a) from Fig. 5(a), (b) from Fig. 5(e).

#### IV. VARIABLE FREQUENCY CARRIER BANDS

A method that could control or at least predict the number of switchings that occur at each level in a multilevel inverter would be advantageous. To accomplish this objective in a multilevel voltage source inverter that has a sine wave reference, knowledge of how long the reference dwells in each of the carrier time bands is required. The following section details how this information is obtained.

##### A. SH-PWM

In carrier based multilevel PWM, the number of carrier bands is one less than the number of voltage levels  $m$  as shown in Fig. 8(a) for an inverter with an odd number of bands (even number of levels) and in Fig. 8(b) for an inverter with an even number of bands (odd number of levels). For a sine wave modulation (reference) waveform centered in the carrier bands (SH-PWM), the duration of time that the waveform exists during each of the bands occupied can be computed as follows. Using the amplitude symmetry of the sinewave about the time axis, the band crossing times  $t_n$ , where the reference waveform crosses from one band to an adjacent band, for bands above (or containing the zero axis in the case that  $m$  is even) can be computed from (6).

$$t_n = \arcsin \left( \frac{2 \cdot n - \text{mod} \left( \frac{m-1}{2} \right)}{m_a \cdot (m-1)} \right), n = 0, 1, 2, \dots \left[ \frac{m}{2} - 1 \right], \quad (6)$$

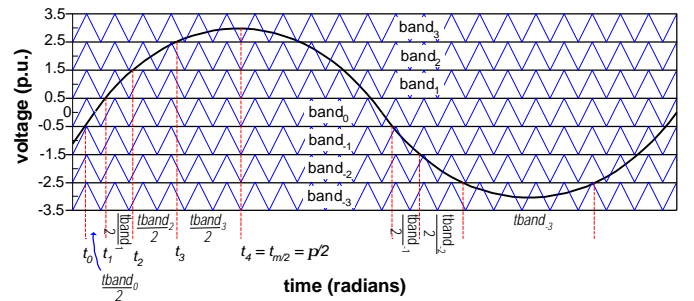
where  $\text{mod}(x/y)$  is the modulus operator. Also noting that the sinewave has a maximum amplitude at  $\pi/2$ , this is set equal to  $t_{\lfloor \frac{m}{2} \rfloor}$ . From (6), the band dwell times in radians (starting at the band adjacent to the zero axis in the case that  $m$  is odd or the band occupying the zero axis in the case that  $m$  is even) are then calculated:

$$t_{band_n} = 2 \cdot (t_{n+1} - t_n), \text{ where } n = 0, 1, 2, \dots, \left[ \frac{m}{2} - 1 \right]. \quad (7)$$

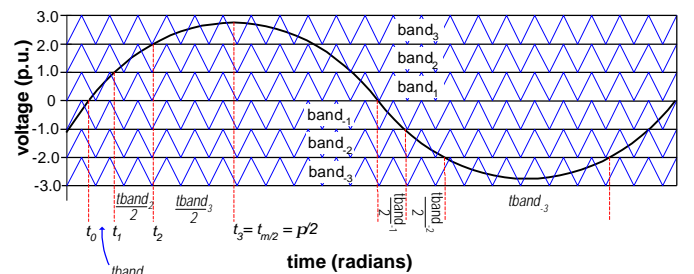
Because of the symmetry of the sinewave about the zero axis, the bands below the zero axis are simply

$$t_{band_{-n}} = t_{band_n}. \quad (8)$$

The number of switchings per modulation cycle at each level of the inverter is dependent on the carrier frequency for that level and the duration of time that the reference waveform dwells within the level's corresponding time band. If the carrier frequency for all of the levels is identical, the top and bottom levels will have many more switchings than the intermediate levels as shown in the previous section.



(a) odd number of carrier time bands ( $m$  is even)



(b) even number of carrier time bands ( $m$  is odd)

Fig. 8. SH-PWM reference dwell times for individual carrier bands.

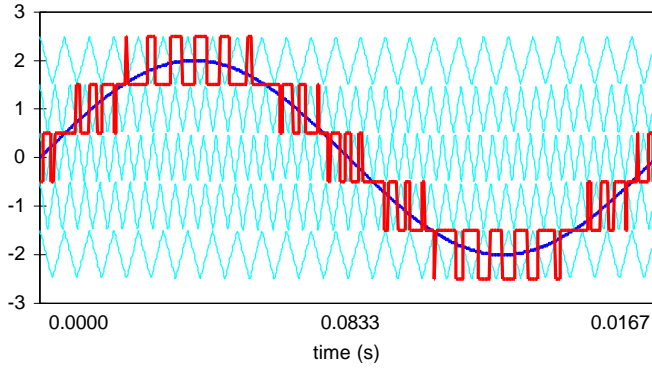


Fig. 9. SH-PWM where carriers have different frequencies ( $m_f = 25$  for Band<sub>2</sub>, Band<sub>2</sub>;  $m_f = 41$  for Band<sub>1</sub>, Band<sub>1</sub>;  $m_f = 49$  for Band<sub>0</sub>).

One method to balance the number of active switchings among the levels is to vary the carrier frequency of each band based on the time duration that the reference waveform dwells during the time band. The relationship between the number of switchings per band,  $N_{sw_n}$ , and the frequency ratio,  $m_{f_n}$ , for each band  $n$  of an inverter is approximately given as follows:

$$m_{f_n} = \frac{P \cdot N_{sw_n}}{t_{band_n}} = \frac{P \cdot N_{sw_n}}{2 \cdot (t_{n+1} - t_n)}. \quad (9)$$

From (9) and solutions to (7) and (8), the frequency ratio  $m_{f_n}$  for each band can be set such that each of the levels in the inverter has approximately the same number of active device switchings per cycle, i.e.,  $N_{sw_n}$  is the same for all levels. Fig. 9 shows an example of the carrier waves and resulting output voltage from this control where  $N_{sw_n}$  has been set to 12.

### B. SFO-PWM

To control the number of switchings in a multilevel inverter that is using SFO-PWM, different equations are needed to calculate the time duration that a sine wave reference waveform with zero sequence addition dwells in each band. Fig. 10(a) shows the carrier bands and reference waveform for multilevel SFO-PWM control. From this figure, one can see that the modulation waveform contains two segments that can be closely approximated as straight lines. Each of these line segments have a horizontal time duration of  $\pi/3$  radians and a vertical amplitude of  $0.75 \cdot m_a \cdot (m-1)$ . Using the properties of proportional triangles from the enlarged area shown in Fig. 10(b), the following equations result:

$$\frac{t_{line}}{P/3} = \frac{\text{int}(0.75 \cdot m_a \cdot (m-1))}{0.75 \cdot m_a \cdot (m-1)}, \text{ and} \quad (10)$$

$$t_{band_n} = t_{band_{-n}} = \frac{t_{line}}{\text{int}(0.75 \cdot m_a \cdot (m-1))}, \quad (11)$$

$$\text{where } n = 0, 1, 2, \dots, \left\lfloor \frac{\text{int}(0.75 \cdot m_a \cdot (m-1))}{2} \right\rfloor.$$

The two ‘‘humps’’ at the top and bottom of the SFO-PWM modulation waveform each have a time duration of  $2\pi/3$  radians. Considering the case where the two humps are wholly contained within a time band, the time duration that the modulation waveform dwells within these two bands can be given as

$$t_{band_{n+1}} = t_{band_{-(n+1)}} = \frac{2P}{3} + \frac{1}{2} \left( \frac{P}{3} - t_{line} \right), \quad (12)$$

where  $n$  is the maximum value used in (11).

Once the duration of dwell time for each of the carrier bands is known, (9) can be used to balance the number of switchings per modulation cycle among the levels of the inverter.

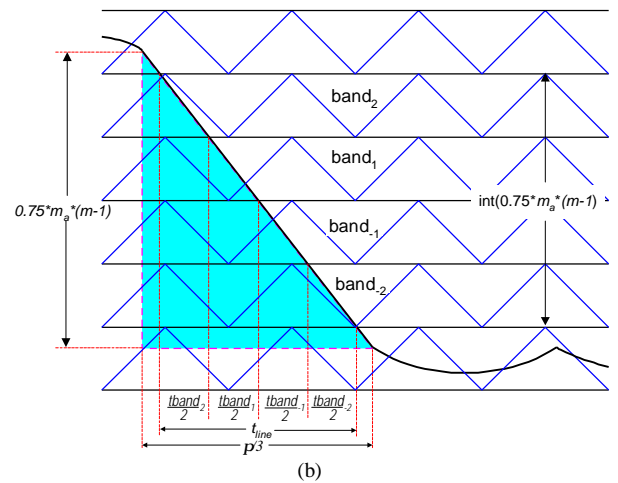
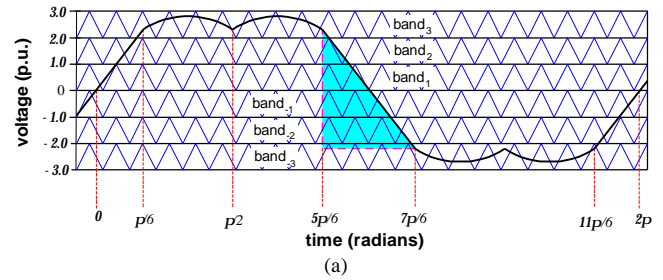


Fig. 10. Carrier bands for a 7-level inverter with SFO-PWM. (a) Modulation waveform and carrier bands. (b) Expanded view of straight segment.

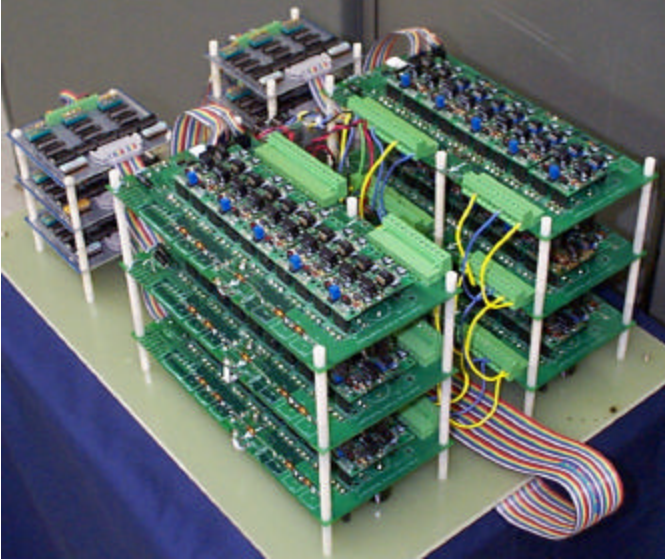


Fig. 11. Prototype 6-level, 10 kW back-to-back diode clamped converter.

## V. HARDWARE IMPLEMENTATION

A 6-level three-phase back-to-back 10 kW converter prototype, pictured in Fig. 11, has been built for operation at a line voltage of 208V for use as an adjustable speed drive for an induction motor [16]. The active switching devices used for the converter were 100 V, 50 A MOSFETs. Each internal dc level of the converter had a capacitance of 6.72 mF.

The inverter was first controlled with SFO-PWM with the following parameters:  $m_a = 1.0$ ,  $m_f = 21$ , and  $f = 0.15$  rad. The inverter's output line-neutral voltage waveforms for all three phases are shown in Fig. 12(a), and the line-line voltage waveform,  $V_{Lab}$ , is shown in Fig. 12(b). From the line-neutral waveforms, one can see that the top and bottom active devices on each phase switch 16 times per modulation cycle whereas the intermediate devices only switch 6 times per modulation cycle.

The prototype inverter was also controlled using carrier bands with different carrier frequencies as discussed in section IV of this paper. Specifically, the top and bottom bands had a frequency index of 11, while the intermediate bands had a frequency index of 53. The phase displacement angle ( $f = 0.15$  rad) and amplitude modulation index ( $m_a = 1.0$ ) were not changed from the example shown in Fig. 12. Fig. 13 shows the inverter's output line-neutral and line-line voltage waveforms when using this type of control method. All of the active devices in the inverter switch states either 8 or 10 times per modulation cycle.

The total harmonic distortion of the line-line voltage waveform in Fig. 12(b) is 4.0%, and no individual harmonic component has a magnitude greater than 1.3% of the fundamental. The THD of the line-line voltage waveform in Fig. 13(b) is 11.6%.

For this particular example, the control scheme balanced the number of device switchings but increased the distortion in the inverter's output voltage. However, because a sinusoidal line-line voltage is the desired waveform for most motor drives, an algorithm can be written to determine a priori the minimum harmonic distortion for a given amplitude modulation index and desired switch utilization by combining the procedures outlined previously in sections III and IV.

## VI. CONCLUSIONS

Multilevel carrier-based PWM offers many more degrees of freedom than traditional two-level PWM. In multilevel PWM, the switching frequency can be less than or greater than the carrier frequency and is a function of the displacement phase angle between the carrier set and the modulation waveform. By adjusting the displacement phase angle in multilevel PWM switching strategies, switching losses can be minimized for a more efficient multilevel inverter.

In traditional subharmonic PWM and switching frequency optimal PWM, the top and bottom switches are switched much more often than the intermediate devices. A novel method to balance device switchings for all of the levels in a diode clamped inverter has been demonstrated for SH-PWM and SFO-PWM by varying the frequency for the different triangle wave carrier bands.

A 6-level back-to-back diode clamped converter prototype has established that these novel carrier-based switching strategies can be used to enable better switch utilization. The need for an algorithm to combine the two procedures studied (changing the phase displacement angle and varying the frequency of the carrier bands) has been identified.

## REFERENCES

- [1] A. Nabae, I. Takahashi, H. Akagi, "A New Neutral-Point-Clamped PWM Inverter," *IEEE Trans. Industry Applications*, vol. IA-17, no. 5, Sept. 1981, pp. 518-523.
- [2] J. K. Steinke, "Control Strategy for a Three Phase AC Traction Drive with a 3-Level GTO PWM Inverter," *IEEE PESC*, 1988, pp. 431-438.
- [3] G. Carrara, S. Gardella, M. Marchesoni, R. Salutari, G. Sciutto, "A New Multilevel PWM Method: A Theoretical Analysis," *IEEE Trans. Power Electronics*, vol. 7, no. 3, July 1992, pp. 497-505.
- [4] R. W. Menzies, P. Steimer, J. K. Steinke, "Five-Level GTO Inverters for Large Induction Motor Drives," *IEEE Trans. Industry Applications*, vol. 30, no. 4, July 1994, pp. 938-944.
- [5] R. W. Menzies, Y. Zhuang, "Advanced Static Compensation Using a Multilevel GTO Thyristor Inverter," *IEEE Trans. Power Delivery*, April 1995, pp. 732-738.
- [6] Y. Chen, B. Mwinyiwiwa, Z. Wolanski, B. T. Ooi, "Regulating and Equalizing DC Capacitance Voltages in Multilevel STATCOM," *IEEE Trans. Power Delivery*, vol. 12, no. 2, April 1997, pp. 901-907.
- [7] N. S. Choi, J. G. Cho, G. H. Cho, "A General Circuit Topology of Multilevel Inverter," *IEEE PESC*, 1991, pp. 96-103.

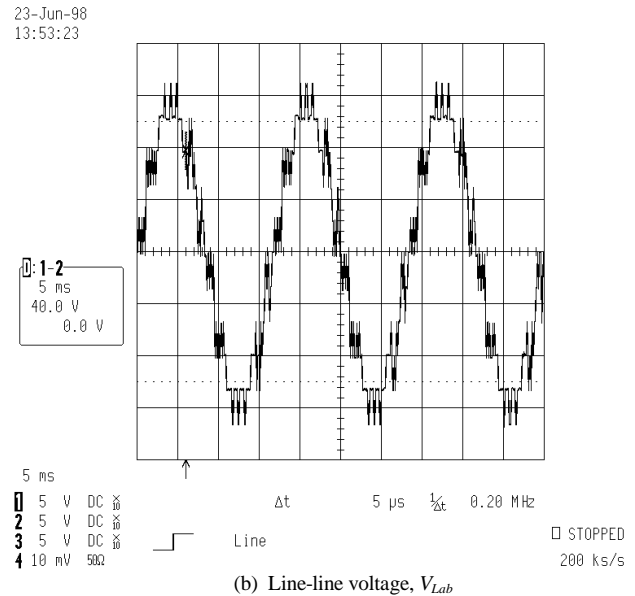
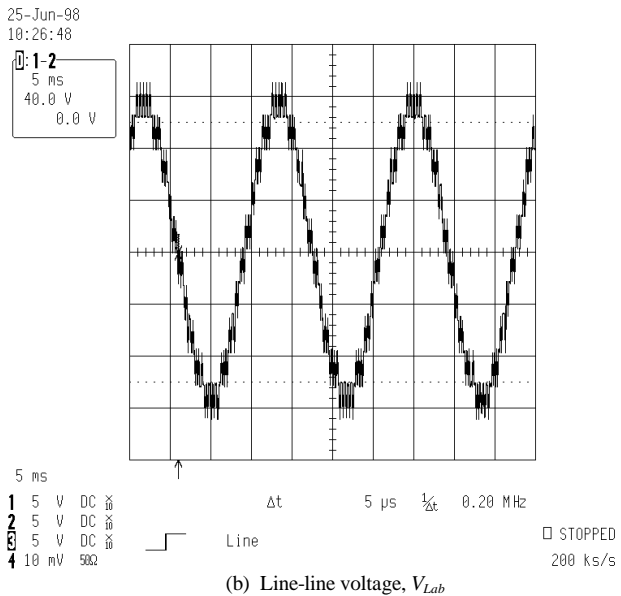
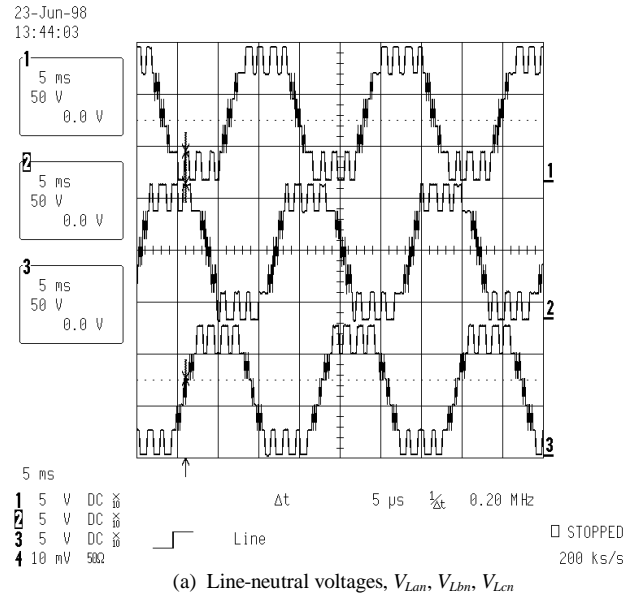
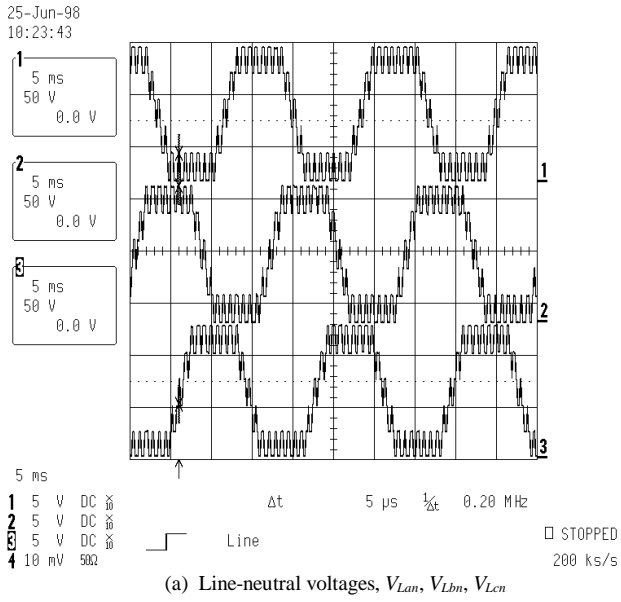


Fig. 12. Experimental voltage waveforms for output of prototype converter controlled with same frequency carrier-bands. ( $m_a = 1.0$ ,  $\hat{f} = 0.15$  rad,  $m_f = 21$  for all bands)

Fig. 13. Experimental voltage waveforms for output of prototype converter controlled with variable frequency carrier-bands. ( $m_a = 1.0$ ,  $\hat{f} = 0.15$  rad,  $m_f = 11$  for top and bottom bands,  $m_f = 53$  for intermediate bands)

- [8] N. S. Choi, G. C. Cho, G. H. Cho, "Modeling and Analysis of a Static Var Compensator Using Multilevel Voltage Source Inverter," *IEEE IAS Annual Meeting*, 1993, pp. 901-908.
- [9] V. G. Agelidis, M. Calais, "Application Specific Harmonic Performance Evaluation of Multicarrier PWM Techniques," *IEEE PESC*, 1998, pp. 172-178.
- [10] M. Fracchia, T. Ghiara, M. Marchesoni, M. Mazzucchelli, "Optimized Modulation Techniques for the Generalized N-Level Converter," *IEEE PESC*, 1992, pp. 1205-1213.
- [11] H. L. Liu, G. H. Cho, "Three-Level Space Vector PWM in Low Index Modulation Region Avoiding Narrow Pulse Problem," *IEEE Trans. Power Electronics*, vol. 9, no. 5, Sept. 1994, pp. 481-486.
- [12] G. Sinha, T. A. Lipo, "A Four Level Rectifier-Inverter System for Drive Applications," *IEEE IAS Annual Meeting*, 1996, pp. 980-987.
- [13] M. H. Ohsato, G. Kimura, M. Shioya, "Five-Stepped PWM Inverter Used in Photovoltaic Systems," *IEEE Trans. Industrial Electronics*, vol. 38, no. 5, Oct. 1991, pp. 393-397.
- [14] G. Carrara, D. Casini, S. Gardella, R. Salutati, "Optimal PWM for the Control of Multilevel Voltage Source Inverter," *Fifth Annual European Conference on Power Electronics*, vol. 4, 1993, pp. 255-259.
- [15] D. G. Holmes, "The Significance of Zero Space Vector Placement for Carrier Based PWM Schemes," *IEEE IAS Annual Meeting*, 1995, pp. 2451-2458.
- [16] L. M. Tolbert, F. Z. Peng, "Multilevel Converters for Large Electric Drives," *IEEE APEC*, 1998, pp. 530-536.